JAAS

Accepted Manuscript

This is an *Accepted Manuscript*, which has been through the Royal Society of Chemistry peer review process and has been accepted for publication.

Accepted Manuscripts are published online shortly after acceptance, before technical editing, formatting and proof reading. Using this free service, authors can make their results available to the community, in citable form, before we publish the edited article. We will replace this *Accepted Manuscript* with the edited and formatted *Advance Article* as soon as it is available.

You can find more information about *Accepted Manuscripts* in the Information for Authors.

Please note that technical editing may introduce minor changes to the text and/or graphics, which may alter content. The journal's standard Terms & Conditions and the Ethical guidelines still apply. In no event shall the Royal Society of Chemistry be held responsible for any errors or omissions in this *Accepted Manuscript* or any consequences arising from the use of any information it contains.

ROYAL SOCIETY OF CHEMISTRY

www.rsc.org/jaas

ARTICLE TYPE www. rsc.org/xxxxxx | XXXXXXXX

An infrared spectroscopic study of the nature of zinc carboxylates in oil paintings†

Joen J. Hermans,* Katrien Keune, Annelies van Loon and Piet D. Iedema

Received Xth XXXXXXXXXX 20XX, Accepted Xth XXXXXXXXX 20XX
First published on the web Xth XXXXXXXXXX 200X
DOI: 10.1039/b000000x

The formation of metal soaps is a major problem for oil paintings conservators. The complexes of either lead or zinc and fatty acids are the product of reactions between common pigments and the oil binder, and they are associated with many types of degradation that affect the appearance and stability of oil paint layers. Fourier transform infrared spectroscopy (FTIR) reveals that a paint sample from *The Woodcutter (after Millet)* by Vincent van Gogh contains two distinct zinc carboxylate species, one similar to crystalline zinc palmitate and one that is characterized by a broadened asymmetric stretch COO^- band shifted to 1570-1 590 cm^{-1}. This observation has been made in many paintings. Although several hypotheses exist to explain the shifted broad carboxylate band, these were not supported by experimental evidence. In this paper, experiments were carried out to characterize the second zinc carboxylate type. It is shown that neither variations in the composition of zinc soaps (i.e. zinc soaps containing mixtures of fatty acids or metals) nor fatty acids adsorbed on pigment surfaces are responsible for the second zinc carboxylate species. X-ray diffraction (XRD) and FTIR analysis indicate that the broad COO^- band represents amorphous zinc carboxylates. These species can be interpreted as either non-crystalline zinc soaps or zinc ions bound to carboxylate moieties on the polymerized oil network, a system similar to ionomers. These findings uncover an intermediate stage of metal soap-related degradation of oil paintings, and lead the way to improved methods for the prevention and treatment of oil paint degradation.

1 Introduction

From a chemical point of view, oil paintings are not stable objects. The drying oil that acts as binding medium in the oil paint, usually linseed oil, polymerizes in a matter of weeks[1], but long-term degradation processes take place over the course of centuries that affect the appearance and structural integrity of the painting. A prominent issue for paintings conservators is the formation of metal soaps. The presence of metal soaps has been reported for numerous paintings ranging from Rembrandt in the 17th century to Salvador Dalí in the 20th century[2–11]. These complexes of either lead or zinc with stearic and/or palmitic acid are the consequence of reactions between the common pigments lead white ($2\,PbCO_3 \cdot Pb(OH)_2$), red lead (Pb_3O_4), lead-tin yellow (Pb_2SnO_4) or zinc white (ZnO) and the oil binder. Metal soaps defects may appear in the paint system in many different forms: as large aggregates that deform paint layers, as deposits on the surface of a paint or homogeneously spread throughout paint layers. Besides causing a loss of pigment and a change in surface texture, the formation of metal soaps has been linked to cases of brittleness, loss of strength and delamination of paint layers.

The variation in metal soap appearance and location within the paint suggests a complex set of processes by which metal soaps form and separate from the paint matrix. However, the chemical reactions that lead to metal soap formation and the transport mechanisms for the reactants and products in these reactions are not fully understood. Answering these questions is a challenging task because of the limited availability of sample material from real paintings and the difficulty of reproducing all the different states of degradation that a painting might be in. A full understanding of metal soap related phenomena in oil paintings must start with an accurate analysis of the molecular structure of metal soaps and all the variations that might be found in oil paint systems. Ultimately, we need to be able to describe the composition and structure of an oil paint on a molecular level in terms of, for instance, concentrations of functional groups, polymerization degree, cross-link density and metal content. Only then, it is possible to investigate how paint composition and environmental factors affect the degree of metal soap related degradation of a painting and finally to develop conservation strategies that minimize the chance of further paint degradation.

Fourier transform infrared (FTIR) spectroscopy is a powerful technique to identify metal soaps in cross-sections of oil paintings. The position and shape of the asymmetric

† Electronic Supplementary Information (ESI) available: Time-dependent ATR-FTIR spectra and XRD traces of the ZnUFA complex, d-spacing of $ZnC_{16}C_{18}$ mixtures, and additional FTIR spectra of Zn-pol and ZnO-LO systems. See DOI: 10.1039/b000000x/

Van 't Hoff Institute for Molecular Sciences, University of Amsterdam, PO box 94157, 1090GD Amsterdam, The Netherlands. Tel: +31 (0)20 525 6442; E-mail: j.j.hermans@uva.nl

stretch vibration band of the carboxylate group in the metal soap (ν_a COO^-) is characteristic for the type of metal ion, e.g. a single sharp band at 1 536 cm^{-1} for zinc soaps[12,13]. Though it is known that metal soaps formed in oil paint layers contain mostly stearic and palmitic acid[4,12], the FTIR spectra of metal soaps formed in paints often do not match with the metal stearates or palmitates synthesized as references. Specifically, the ν_a COO^- band is frequently significantly broadened and shifted to higher wavenumbers (between 1570 and 1 590 cm^{-1}) in ZnO containing paint layers[7,9,14–17]. We discuss Attenuated Total Reflection Fourier Transform infrared microscopy (μ-ATR-FTIR) analysis of a sample from the painting *De Houthakker (naar Millet)* ('The Woodcutter (after Millet)') by Vincent van Gogh as a clear example of this phenomenon.

Several explanations have been suggested to account for the variation in the ν_a COO^- band in zinc white paints. In crystalline zinc palmitate ($Zn(C_{16})_2$), the zinc atoms are surrounded by four equivalent carboxylate groups[18], giving rise to a single sharp ν_a COO^- band in the FTIR spectrum. The broadening of carboxylate band suggests that there is increased variation in the local environment of the carboxylate groups. We have synthesized a range of zinc soaps that contain various mixtures of carboxylic acids or mixtures of metals to study the effect of added complexity in the zinc soap structure on the carboxylate coordination. Secondly, the adsorption of fatty acids on ZnO surfaces has been suggested as an explanation for the broad ν_a COO^- band in FTIR spectra[14,15]. The effect of different binding modes of carboxylic acids on the surface of ZnO particles has been studied by Lenz et al.[19] While it is likely that the energies of COO^- vibrations are not identical in $Zn(C_{16})_2$ and fatty acids adsorbed on ZnO surfaces, it is not clear whether the concentration of surface-bound fatty acids is large enough to cause the entire ν_a COO^- band to shift in paint layers that have a high concentration of zinc carboxylates. We investigated this effect by following the reaction of ZnO powder in a solution of palmitate ions. Lastly, we considered the possibility that there is disorder in the alkyl chains of zinc soap phases that form in ZnO containing paints, by studying the crystallinity of zinc carboxylates formed in a model paint system and zinc containing linseed oil polymers. Dreveni et al. found that the position and shape of the COO^- vibration bands are strongly dependent on the ability of the alkyl chains to interact and pack into a well-ordered lattice[20]. While the fatty acid chains are neatly packed in an all-*trans* fashion in crystalline $Zn(C_{16})_2$[18,21], chains might not have sufficient mobility to pack in a well-ordered manner when zinc soaps form in a polymerized oil network.

This work aims to give a complete overview of the different molecular structures of zinc carboxylates that may be found in oil paint samples. Applying a combination of Fourier transform infrared spectroscopy (ATR-FTIR) and X-ray diffraction (XRD), the effect of relatively minor changes to metal soap composition or physical state can be investigated and detailed structures can be resolved. Finally, we applied the obtained information on the likely structures of zinc carboxylates to develop an hypothesis on the different stages of metal soap formation in oil paint and the transport processes that are involved.

2 Experimental

2.1 Synthesis of zinc soaps

Zinc palmitate ($Zn(C_{16})_2$) and zinc palmitate/stearate ($ZnC_{16}C_{18}$) were synthesized by mixing basic aqueous solutions of the fatty acids with a solution of zinc nitrate. Mixed-metal soaps were prepared by using a solution of NaOH to dissolve palmitic acid ($ZnNa_2(C_{16})_4$), or by melting stochiometric amounts of $Zn(C_{16})_2$ and KC_{16} under inert atmosphere ($ZnK_2(C_{16})_4$). All these procedures are described in detail in Ref.[18]. All zinc soaps were thoroughly dried before analysis either by placing samples in an oven at 110 °C or in a desiccator over P_2O_5, and their purity was confirmed by FTIR and XRD. In experiments where the reaction between ZnO and palmitic acid was followed, ZnO powder was added to an aqueous solution of palmitic acid containing an excess of triethylamine. Samples were taken after 15 seconds and then every 2 minutes. The solid fractions were immediately separated by vacuum filtration and dried in an oven at 110 °C.

To synthesize zinc soaps of unsaturated fatty acids (UFAs), cold-pressed untreated linseed oil (Kremer Pigmente) was hydrolized using an excess of a concentrated aqueous solution of KOH. After neutralization with concentrated HCl, the fatty acid mixture was extracted with dichloromethane and dried with $MgSO_4$. Evaporation of the solvent yielded a clear brown liquid mixture of 53 % linolenic, 19 % linoleic, 16 % oleic, and 12 % stearic and palmitic acid (composition determined by ^{1}H-NMR and ^{13}C-NMR). Zinc soaps of this fatty acid mixture (ZnUFA) were prepared by mixing stoichiometric amounts of zinc nitrate and UFAs in a 1:1 mixture of ethanol and diethyl ether containing and excess amount of triethylamine. After approximately one hour, the solvent was evaporated to yield an off-white product with a pasty texture.

2.2 Preparation of model paint film (ZnO-LO)

The composition of the model paint system was adapted in an attempt to promote the rapid formation of zinc carboxylates, i.e. a high oil/pigment ratio and an addition of water to the paint mixture. Model paint films were prepared by stirring 3.0 g cold-pressed untreated linseed oil (Kremer Pigmente) with 0.5 g ZnO (Sigma-Aldrich) and 1 mL demineralized water in a sealed vial at room temperature for three days. After

allowing the mixture to settle, a few drops of the oil layer were spread on a glass slide and left to dry in air at room temperature for up to seven weeks.

2.3 Preparation of zinc ionomer (Zn-pol)

Zinc sorbate was prepared by dissolving 550 mg sorbic acid with 1 mL triethylamine in 20 mL demineralized water at 50 °C. The addition of 1.0 g $Zn(NO_3)_2 \cdot 6\,H_2O$ dissolved in 5 mL water resulted in immediate precipitation of the white product. After stirring for 20 minutes, the product was separated by vacuum filtration and dried over P_2O_5.

A ionomer film was made by mixing 55 mg zinc sorbate with 200 mg cold-pressed untreated linseed oil, and spreading the resulting turbid paste thinly on a glass plate. After curing at 150 °C in air overnight, a homogeneous yellow transparent polymer film was obtained.

2.4 Analysis

A small sample of *The Woodcutter (after Millet)* by Vincent van Gogh (Figure 1) was embedded in a polyester resin block. The resin block was sanded down and polished until the cross-section was situated on the surface of the block.

Optical analysis was carried out using a Zeiss Axioplan 2 equipped with both a polarized light source and a UV light source (365 nm).

Scanning electron microscopy was performed with a JEOL JSM 5910 LV microscope. Backscattered-electron images (SEM-BSE) were mostly taken at 20 kV accelerating voltage at a 10 mm eucentric working distance. Samples were gold coated to improve surface conductivity.

Cross-sections were analyzed with μ-ATR-FTIR using a Perkin Elmer Spectrum 100 FTIR spectrometer combined with a Spectrum Spotlight 400 FTIR microscope equipped with a 16x1 pixel linear MCT array detector at 8 cm^{-1} resolution. A Perkin Elmer ATR Ge crystal accessory was used for ATR imaging. Spectra were collected in a 600-4 000 cm^{-1} range and averaged over 2 scans.

ATR-FTIR spectra of bulk material were collected on a Varian 660-IR FT-IR spectrometer combined with a Pike Technologies diamond GladiATR unit with 4 cm^{-1} resolution. Spectra were collected in a 600-3 500 cm^{-1} range and averaged over 16 scans.

XRD was performed on a Rigaku MiniFlex II desktop X-ray diffractometer with Cu Kα radiation (λ = 1.541 80 Å) at 30 kV and 15 mA. The equipment was fitted with a Ni Kβ suppression filter. Diffractograms were recorded in a 2θ = 1–40° range (2.5°/min scan rate and 0.025° step size). Powder samples were finely ground with mortar and pestle, and manually pressed into glass sample holders. Model paint films prepared on glass slides were lifted from their support and measured on the underside, since a transparent oil layer formed on top of the film.

3 Results and discussion

3.1 Painting cross-section analysis

The painting *The Woodcutter (after Millet)* was painted by Vincent van Gogh in 1889 (Figure 1). A small sample was taken of the light green paint near the top of the painting. Images of this sample obtained with optical microscopy and SEM microscopy are shown in Figure 2. A previous study showed that the paints Van Gogh used in this section of the painting contain a large variety of pigments. In the ground layers, a mixture of lead white, calcium carbonate, barium sulfate, ochre pigments and a little carbon black was found. The thick light green paint layer shown here contains mostly ZnO, and a mixture of emerald green ($Cu(CH_3COO)_2 \cdot 3\,Cu(AsO_2)_2$) and chrome green ($Cr_2O_3$) or viridian ($Cr_2O_3 \cdot 2\,H_2O$)[22].

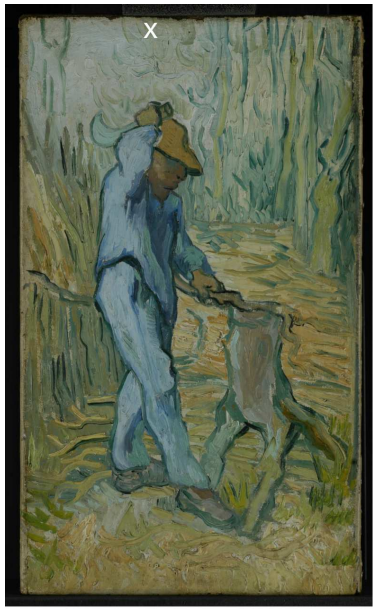

Fig. 1 *De Houthakker (naar Millet)* ('The Woodcutter (after Millet)') by Vincent van Gogh, 1889, 44 cm x 26.2 cm, Van Gogh Museum (Vincent van Gogh Foundation). X marks the spot where the sample shown in Figure 2 is taken.

Analysis of the paint cross-section with μ-ATR-FTIR revealed that the light green paint layer contains a high concentration of zinc carboxylates, as indicated by ν_a COO^- bands in the 1500-1 600 cm^{-1} region. There was considerable variation in the position and width of the carboxylate bands. Figure 2c shows a map of integrated intensity of the sharp band

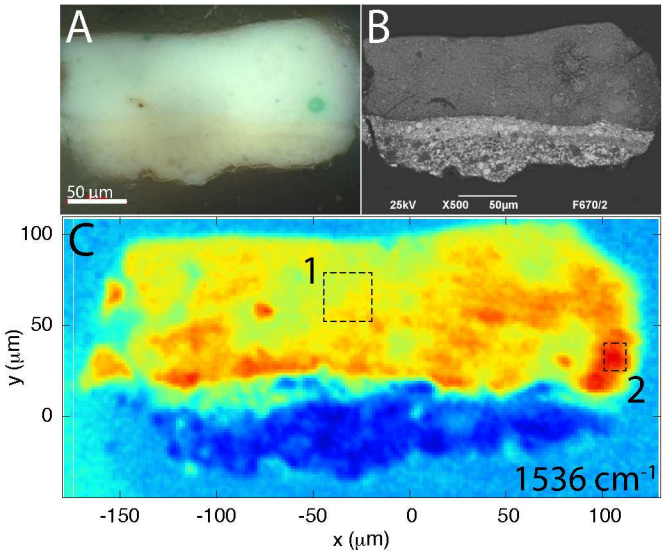

Fig. 2 Paint cross-section from *The Woodcutter (after Millet)* by Vincent van Gogh, showing a thick light green pain rich in ZnO on top of two ground layers. (A) Optical microscopy image, (B) SEM-BSE image and (C) µ-ATR-FTIR map of the sharp band at 1 536 cm^{-1} (integrated between 1495-1 546 cm^{-1}, red color signifies high intensity). Numbers 1 and 2 mark the averaged areas of the FTIR spectra in Figure 3.

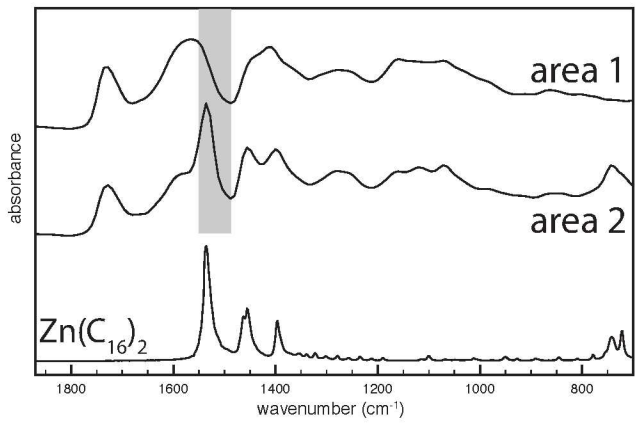

Fig. 3 Averaged µ-ATR-FTIR spectra measured at the two areas in the cross-section of a zinc white paint layer of *The Woodcutter (after Millet)* by Vincent van Gogh, as shown in Figure 2. The grey area marks the wavenumber range integrated to create the zinc carboxylate map in Figure 2. The bottom spectrum of zinc palmitate is included as a reference.

at 1 536 cm^{-1}. A representative spectrum made by averaging the spectra in region 2 is shown in Figure 3. This spectrum closely resembles a reference spectrum of zinc palmitate, with a sharp ν_a COO^- band at 1 536 cm^{-1} and well-defined δ CH_2 and ν_s COO^- bands at 1 450 cm^{-1} and 1 400 cm^{-1}, respectively. Zinc carboxylate material with a sharp ν_a COO^- band at 1 536 cm^{-1} seems to be more prominent in the lower parts of the paint layer, and almost absent in top 20-30 µm of the paint layer. Throughout the paint layer however, a broad ν_a COO^- band was found with a maximum at 1 570 cm^{-1}, region 1 shown in Figure 3. These spectra suggest that the entire ZnO paint layer is filled with a zinc carboxylate species that causes a broad ν_a COO^- band, while deposits of zinc soap material comparable to zinc palmitate or stearate references are concentrated in the lower section of the paint film.

In the next sections, we explore possible variations in zinc carboxylate structures that could induce a change in carboxylate coordination and cause a broadened and shifted ν_a COO^- band.

3.2 Zinc soaps of varying composition

Pure zinc palmitate and zinc stearate are most often used as reference compounds for FTIR analysis. It is known, however, that both fatty acids occur simultaneously in metal soap aggregates in paint samples[4]. Therefore, a series of zinc soaps containing a mixture of palmitate and stearate in varying ratios was prepared ($ZnC_{16}C_{18}$). A single set of long spacing peaks in XRD analysis indicated that zinc palmitate and zinc stearate form a solid solution at all palmitate/stearate ratios (ESI: Figure S1†). The FTIR spectra of these mixed fatty acid soaps were highly similar for all the palmitate/stearate ratios; a typical spectrum is shown in Figure 4a. The mixing of palmitate and stearate only affected the number and intensity of alkyl chain progression bands in the 1100-1 310 cm^{-1} region[13]. The asymmetric carboxylic stretch vibration at 1 538 cm^{-1} was unaffected by this mixing.

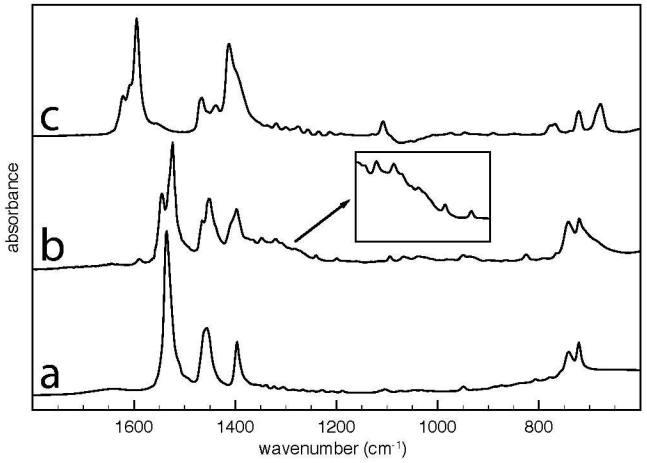

Fig. 4 ATR-FTIR spectra of (a) $ZnC_{16}C_{18}$ (1:1 ratio), (b) ZnUFA and (c) $ZnNa_2(C_{16})_4$.

We have also explored the effect of unsaturations in the fatty acid chains on the structure of zinc soaps. Linseed oil typically contains only 9-13 % saturated fatty acids[1]. In paint samples however, often only zinc soaps of saturated fatty acids are found. It is thought that this occurs because in a fully polymerized oil film, hydrolysis of ester bonds in the tryglycerides leaves only the saturated fatty acids 'free' to diffuse through the oil network. We have fully hydrolyzed linseed oil to yield a mixture of mostly unsaturated fatty acids. The zinc complex of this fatty acid mixture is a crystalline material, as indicated by the presence of progression bands in the FTIR spectrum in the 1100-1 310 cm^{-1} region (Figure 4b) and a strong series of long spacing peaks in the XRD trace (ESI: Figure S2[†]). This monocrystallinity is quite surprising, given the low melting point of unsaturated fatty acids and the heterogeneity of the fatty acid mixture. With a split ν_a COO^- band at 1 545 cm^{-1} and 1 524 cm^{-1}, the FTIR spectrum is very similar to that of zinc oleate and zinc linoleate[12]. Possibly, the presence of *cis* double bonds in the unsaturated fatty acid chains causes a slight asymmetry in the tetrahedral coordination of carboxylic oxygens around the zinc atoms. However, this minor effect is not capable of explaining the extensive band broadening that was observed in the Van Gogh paint sample.

Additionally, we investigated whether the structure of Zn-UFA soaps changes as the non-conjugated double bonds in the fatty acid chains undergo auto-oxidation reactions with atmospheric oxygen to form peroxides, hydroxides and cross-links[23]. A 0.5 mm layer of ZnUFA was left to cure in air at room temperature for up to seven months. In that time, the ν C=CH band at 3 008 cm^{-1} decreased and a broad -OH band appeared around 3 400 cm^{-1}. The ν_a COO^- band was not affected by ageing (ESI: Figure S3[†]). XRD measurements showed clearer changes to the structure, with a decreasing order in the carbon chain packing and a small but significant decrease in the long spacing of 0.6 Å (ESI: Figure S2 and Figure S4[†]).

The last variation in the composition of zinc soaps we investigated is the incorporation of multiple metals. It was found that a different type of zinc soaps can form in linseed oil when a source of sodium or potassium is present such as NaOH or KCl. The synthesis and structure of these alternative soap complexes ($ZnNa_2(C_{16})_4$ and $ZnK_2(C_{16})_4$) is described in detail in Ref.[18]. Concerning the FTIR of these mixed-metal soaps, there is a major shift of the ν_a COO^- band from 1 540 cm^{-1} to 1 595 cm^{-1} with two bands of lower intensity appearing at 1 609 cm^{-1} and 1 620 cm^{-1} for both the sodium and the potassium containing complexes (Figure 4c). Though the band maximum is shifted it is still sharp, in contrast to the band broadening observed in the paint sample of Van Gogh. In comparison to $Zn(C_{16})_2$, this band shift is caused by a transition from bidentate to effectively monodentate carboxylic groups[24]. The split in the ν_a COO^- bands is an effect of the inequivalence of the carboxylic headgroups in the mixed-metal structure, in which half the carboxylate groups bind a zinc and a sodium or potassium atom and half the groups bind two sodium or potassium atoms. Though the mixed-metal soaps can easily be synthesized in a reaction mixture of ZnO, palmitic acid and NaOH/KOH in linseed oil, they have not yet been identified in oil painting samples.

Concluding, none of the variations in zinc soap composition we investigated give a satisfying explanation of the ν_a COO^- band shift and broadening that is often observed in zinc white paint layers.

3.3 ZnO particles in fatty acids solutions

We performed experiments where ZnO powder was added to an aqueous palmitate solution, in an attempt to measure IR absorbance of surface-adsorbed carboxylate molecules. Samples were taken at regular time intervals from 15 s after start of the reaction and analyzed with ATR-FTIR spectroscopy. Figure 5 shows that the height of the characteristic zinc palmitate bands are indeed rising as the reaction progresses. However, the position of the ν_a COO^- band is not affected by the extent of zinc soap formation. Even after just 15 seconds reaction time, when the amount of zinc soap formed is very small and the strength of absorption is very weak, the band has an absorption maximum at 1 536 cm^{-1}. This observation has three possible explanations:

- the ν_a COO^- band of fatty acids adsorbed on ZnO surfaces lies at 1 536 cm^{-1};
- the fatty acid layer directly on the ZnO surface has shifted ν_a COO^- bands, but as soon as IR absorption becomes measurable, the zinc soap phases are already several layers thick and the signal is dominated by the non-shifted bulk zinc soap signal;
- zinc soap formation does not take place on the ZnO surface, but instead it is a precipitation reaction between dissolved Zn^{2+} ions and fatty acids in solution.

We did not investigate which of these explanations is valid, though Taheri et al. did find that myristic acid molecules adsorbed on oxidized zinc surfaces consistently showed sharp ν_a COO^- bands at 1 536 cm^{-1} [25]. However, the situation might be different for an oil paint system where there is a more variation in the molecules with carboxylate functionalities. While we cannot conclude that IR absorption of carboxylates directly adsorbed on a zinc oxide is identical to bulk zinc soaps, this experiment does show that only that if such surface adsorbed species exist in paint systems, their concentration is likely to be too small to account for the entire intensity of the strong ν_a COO^- band that is often measured. In other words,

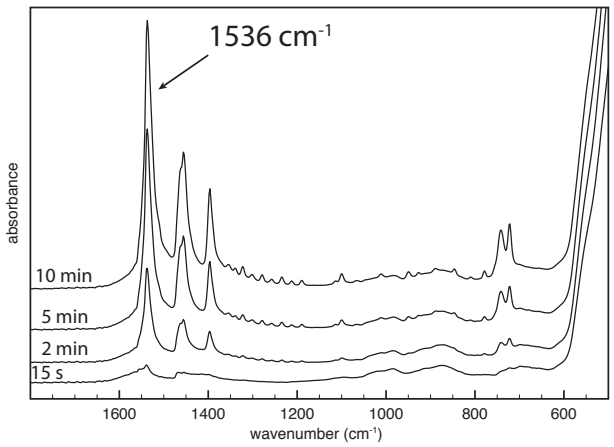

Fig. 5 ATR-FTIR spectra of ZnO immersed in an aqueous palmitate solution for 15 seconds to 10 minutes.

most carboxylates will be residing in bulk zinc soap material, where the effect of the pigment surface does not play a role.

Moreover, we observed the broad shifted ν_a COO^- band in zinc-containing polymerized oil films in which pigment was entirely absent. These crucial experiments are discussed below.

3.4 Disorder in zinc soaps

Next, we discuss disorder in zinc soap structures as an explanation of variations in carboxylate coordination. As mentioned before, in a polymerized oil network fatty acid chains that are to become part of the zinc soap phases might not have sufficient mobility to pack in a well-ordered manner. To investigate whether disorder in the alkyl chain packing affects the coordination of carboxylate groups around the zinc ion, we first considered the FTIR spectrum of molten zinc palmitate (Figure 6b). In the melt, the alkyl chains are completely disorderd, but each carboxylate group is still bound to zinc. Upon melting, the single ν_a COO^- band observed in crystalline zinc palmitate at 1 536 cm^{-1} splits into three bands at 1545, 1593 and 1 633 cm^{-1} at 160 °C, when the complex appears as a clear colorless liquid. Ishioka and co-workers have studied the structural changes associated with this phase transition with EXAFS and concluded that the coordination number and Zn−O bond lengths are the same in both phases[26]. Therefore, the striking changes in the FTIR spectrum of molten zinc palmitate must be due to a geometrical distortion of the tetrahedral coordination structure of the carboxylate groups around the zinc ion, caused by the increased mobility of the molten alkyl chains. The effect of complete disorder in the alkyl chains on the ν_a COO^- vibration is significant. Though the shape of the bands is still different, the chain disorder produces a shift to higher wavenumbers comparable to the spectrum in region 1 from the Van Gogh paint sample (compare Figure 6b and 6c).

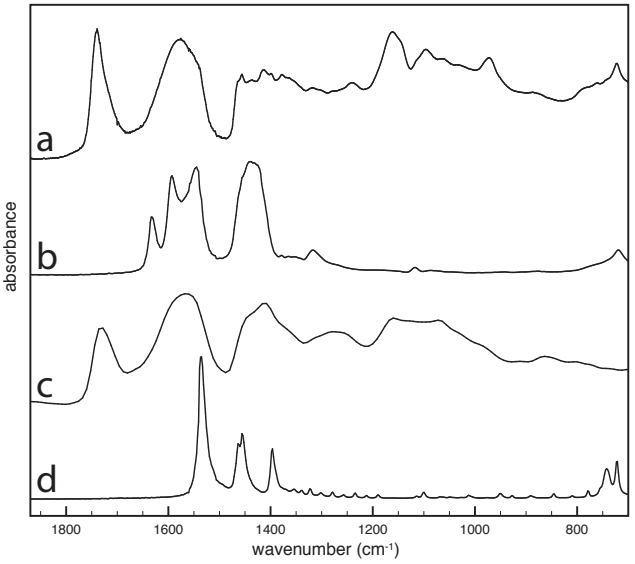

Fig. 6 ATR-FTIR spectra of (a) zinc soaps formed in a cured film of ZnO in linseed oil (ZnO-LO), (b) molten zinc palmitate at 160 °C, (c) area 1 in the sample from Van Gogh's *The Woodcutter (after Millet)* and (d) zinc palmitate at room temperature.

In an attempt to produce disordered zinc soaps in a way more closely related to actual oil paint, we prepared a ZnO 'paint' film designed to promote the fast formation of zinc soaps by using an excess of linseed oil and stirring the paint with water before application. Already after one week, a broad ν_a COO^- band was observed. Figure 6a shows the ATR-FTIR spectrum of the bottom of such a film after 80 days of drying on a glass support (ZnO-LO). The broad ν_a COO^- band centered at 1 575 cm^{-1} is similar to the band from the van Gogh paint in Figure 3 (area 1), though a weak shoulder can be observed around 1 540 cm^{-1}. The intensity of the ν_a COO^- band relative to the ester carbonyl band of the cured oil network at 1 739 cm^{-1} indicates that the concentration of zinc carboxylates in this system is quite high.

It should be remarked that the similarity between the broad ν_a COO^- bands in the Van Gogh paint and in ZnO-LO is a crucial finding (Figure 6a and 6c). It implies that this experiment is one of the few successful attempts to produce a film containing zinc carboxylates with a coordination structure very similar to those found in old paintings on a very short timescale[15]. We proceeded with X-ray diffraction analysis to study the crystalline order in this system.

Figure 7 shows the XRD trace measured on the bottom of the model ZnO paint film ZnO-LO, compared to a linseed oil

film cured with no additives (LO) and a mixture of zinc palmitate and ZnO. The three characterstic peaks of at 31.8°, 34.5° and 36.3° in ZnO-LO show that there is still ZnO present. The broad peak with a maximum around 20° ($d = 4.4$ Å) appears in both the pure linseed oil film and in the model paint. Such a broad peak is often seen in amorphous polymer material and can be associated with the average distance between the carbon chains in the cross-linked oil network[27].

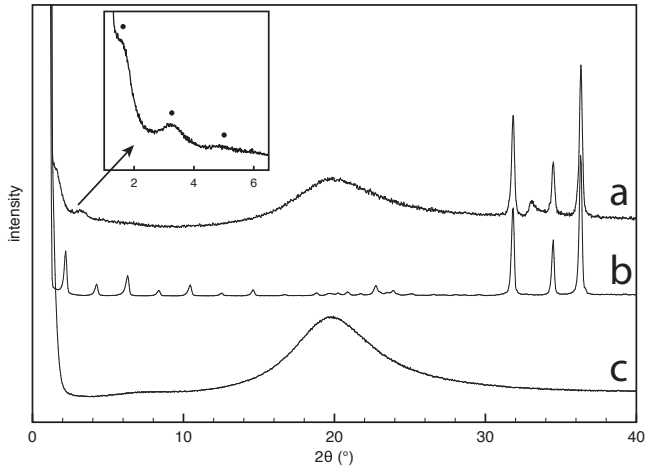

Fig. 7 XRD traces of (a) ZnO-LO, (b) crystalline $Zn(C_{16})_2$ synthesized from ZnO and (c) a pure linseed oil film. Intensities of the three traces are not to scale. The insert shows the three peaks (marked with •) in the low angle section of the XRD trace measured at higher resolution and slower scanning speed.

In Figure 7b at small angles we see the typical series of sharp peaks associated with the long spacing in the bulk crystalline zinc palmitate. In the trace of ZnO-LO, similar peaks appear in the same region at 1.5°, 3.3° and around 5°, though they are significantly broader and much weaker (see inset in Figure 7). These three evenly spaced peaks correspond to the first three diffraction orders of the long spacing in zinc soaps. The width of the peaks shows that the crystalline domains are much smaller than in bulk zinc palmitate. The absence of a well-resolved series of long spacing peaks prevents an accurate calculation of the long spacing, but based on this data the value can be estimated to be around 50 Å. This spacing is significantly larger than the long spacing of a zinc soap that contains both palmitate and stearate ($ZnC_{16}C_{18}$, 41.4 Å for a 1:1 mixture) or zinc soaps containing a mixture of unsaturated fatty acids (ZnUFA, 41.8 Å).

This XRD analysis shows that the ZnO-LO sample contains a very low concentration of small (semi)-crystalline zinc soap particles. This small amount cannot, however, account for the strong ν_a COO^- band in the FTIR spectrum of ZnO-LO (Figure 6). The lack of strong long spacing peaks leads to the conclusion that the zinc carboxylate species associated with the broad ν_a COO^- band around 1 570 cm^{-1} must be amorphous.

Based on the FTIR spectrum and XRD analysis of ZnO-LO, we will now discuss explanations of the observed ν_a COO^- band broadening and shift. Possibly, the zinc carboxylate species are zinc soaps of saturated fatty acids being delayed or hindered in their crystallization process. In a polymerized oil network, thermal movement of fatty acid chains might be constrained by the surrounding oil network, making alignment and proper crystallization of the chains a much slower process than the coordination of zinc ions by fatty acid carboxylate groups. In this scenario, the amorphous state of the fatty acid chains distorts the ideal tetrahedral coordination of the carboxylic groups around the zinc atom in a fashion similar to molten zinc palmitate (Figure 6). If this hypothesis is correct, on a longer timescale it is expected that the degree of crystallization will increase and that a sharp ν_a COO^- band at 1 536 cm^{-1} will appear in the FTIR spectrum of ZnO paint layers. This explanation implies that the observed system is not in thermodynamic equilibrium and is bound to move to a final state of, probably, large well-ordered metal soap crystals.

A second interpretation is that the zinc carboxylate species is not an isolated molecular species present in the paint film, but in fact integral part of the oil network structure. Network carboxylic acid groups may form by hydrolysis of triacyl glycerol ester bonds after polymerization of the fatty acid chains has occurred, or through β-scission reactions and subsequent oxidation in the unsaturated fatty acid chains[23]. The view of the oil network as a polymer chain with carboxylic acid sidechains would make it a complicated type of ionomer. The term "ionomer" refers to ion-containing polymers, typically consisting of a hydrocarbon backbone with a small number of pendant acid groups. In commercial ionomers, these acid group are often partially or completely neutralized by Na^+, Zn^{2+} or other metal ions. The structure of ionomers has been extensively studied. It was found that the ionic groups have a well-defined local structure and cluster to form ion-rich domains within the polymer matrix[28–30]. Interestingly, an ethylene-methacrylic acid copolymer completely neutralized by Zn^{2+} ions shows a relatively broad ν_a COO^- band at 1 585 cm^{-1}, which is similar to the band we observed for the ZnO-LO system[28].

In order to test the ionomer interpretation, we attempted to produce a zinc ionomer from linseed oil. Commonly, ionomers are prepared by letting a polymer that contains ionic groups react with a metal salt in the melt or in solution. Since polymerized linseed oil decomposes before it melts and has a poor solubility in organic solvents, we chose to introduce zinc ions in the polymer matrix by copolymerization. The zinc complex of sorbic acid (2,4-hexadienoic acid, or C6:2) was mixed with linseed oil and cured as a film at 150 °C in air to induce cross-linking between the double bonds of unsaturated triglycerides and the sorbate chains. While zinc sor-

bate did not dissolve in linseed oil, upon curing the mixture of zinc sorbate and linseed oil formed a completely transparent polymer film (Zn-pol), as shown in Figure 8b. Figure 8a compares the FTIR spectra of zinc sorbate and Zn-pol. Upon curing, the three sharp bands of zinc sorbate at 1515, 1620 and 1 645 cm^{-1} disappear and a broad ν_a COO^- band appears with a maximum at 1 585 cm^{-1}. The absence of a C=CH band at 3 008 cm^{-1} indicated that all double bonds in the system were either cross-linked or oxidized (ESI: Figure S5†). The XRD trace in Figure 8c confirms that Zn-pol is amorphous and contains no remaining traces of unreacted zinc sorbate, showing only the broad peak around 20° that was also found in pure linseed oil films. The weak maximum around 6° ($d \approx 15$ Å) proved poorly reproducible and remains to be interpreted.

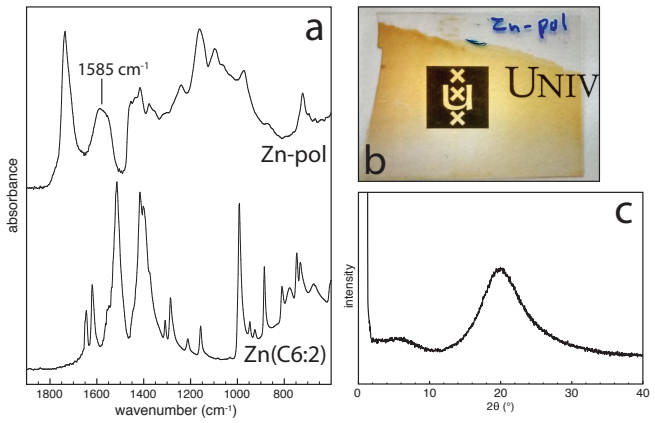

Fig. 8 (a) FTIR spectra of zinc sorbate (Zn(C6:2), bottom) and a cured mixture of zinc sorbate and linseed oil (Zn-pol, top), showing a broad ν_a COO^- band with a maximum at 1 585 cm^{-1}. (b) Photograph of a completely transparent thin yellow film of Zn-pol. (c) XRD trace of Zn-pol.

The FTIR spectrum of the Zn-pol ionomer is strikingly similar to the spectra of both the ZnO-LO system and the Van Gogh paint sample, showing that an amorphous polymer system containing network-bound zinc carboxylate groups is a valid explanation for the shifted broad ν_a COO^- band in oil paints. Moreover, the complete absence of ZnO pigment in this system emphasizes that the zinc carboxylate species corresponding to the broad ν_a COO^- band is not associated with pigment surfaces. This conclusion is further supported by the observation that the broad ν_a COO^- band in the ZnO-LO system also appeared in transparent sections of the paint film that contained no ZnO pigment (ESI: Figure S6†).

Applying our findings to the sample from *The Woodcutter (after Millet)* shown in Figure 2c, it means that amorphous zinc carboxylate species are homogeneously spread throughout the light green paint layer. Crystallization of zinc soaps, as indicated by the sharp 1 536 cm^{-1} band, has occurred mostly in the lower section of the paint layer, and is concentrated in domains rich in zinc soaps. A similar distribution of zinc carboxylate species was also found by Osmond et al. in 40 year old ZnO tube paint films and home-made reconstructions [14], and could be due to an uneven degree of polymerization in the paint layer or an inhomogeneous concentration of 'free' fatty acids.

Based on the results shown here, a clear distinction between disordered zinc soaps or a zinc-neutralized ionomer cannot be made. However, it may be most likely that both types of zinc carboxylate contribute to the broad ν_a COO^- band around 1570-1 590 cm^{-1} that we find in ZnO-LO and in historical zinc white paints. It is often observed that zinc soaps containing mostly saturated fatty acids form spontaneously in oil paint films containing ZnO, and since our system is so similar to paint formulations, there is no reason why they should not be forming at least to some extent in ZnO-LO. In fact, the shoulder in the FTIR spectrum of ZnO-LO at 1 536 cm^{-1} and the weak set of long spacing peaks in the XRD results suggest that there is a low concentration of crystalline zinc soaps present already.

Furthermore, if (semi-)crystalline zinc soap material is nucleating somewhere in the paint system and subsequently increasing in size, there must be transport of Zn^{2+} ions from the ZnO pigment particles to the growing zinc soap aggregate. Since isolated ions are unlikely to exist in a relatively apolar medium like a polymerized oil film, as Zn^{2+} moves through the paint system it needs to be accompanied by a suitable negative countercharge. The most obvious candidates for these countercharges are the carboxylic groups that are part of the polymer network. Diffusion of metal ions in ionomer systems has been studied both experimentally and through molecular simulations [31–34], and was shown to occur through an "ion hopping" mechanism in which metal ions are transferred between ionic groups on different polymer chains. Crucially, this diffusion process only occurs at an appreciable rate when the polymer is heated above its glass transition temperature, when the polymer chains are mobile enough to bring together their ionic groups to a distance where the transfer of ion from one carboxylic group to the other is feasible.

We confirmed to capability of Zn^{2+} ions to exchange between carboxylate groups in linseed oil experimentally. Two days after mixing of two clear linseed oil solutions, one containing ZnUFA and the other palmitic acid, crystalline zinc palmitate could be isolated from the resulting turbid reaction mixture and identified with FTIR spectroscopy. This simple pilot experiment shows that even in an oil environment, the zinc-carboxylate bond may be broken and the precipitation of zinc palmitate drives the exchange of Zn^{2+} ions from dissolved unsaturated fatty acids to saturated fatty acid chains.

If ionomers can indeed be considered valid model systems for aged oil paint, the glass transition temperature of oil paint

and any factor that influences this physical property (e.g. relative humidity, solvent absorption, pigmentation) could become a crucial parameter for the rate of metal ion diffusion and therefore metal soap growth. Further investigations into the preparation of ionomeric systems closely resembling a polymerized oil network and the analysis of these systems to study the relation between diffusion processes in ionomers and oil paint films are the topic of a forthcoming publication.

4 Conclusions

In samples of zinc white paint layers, different types of zinc carboxylates are found. A species characterized by a sharp ν_a COO^- band at 1 536 cm^{-1} corresponds to crystalline zinc soaps of saturated fatty acids, but the nature of a second type characterized by a broad ν_a COO^- band with a maximum between 1570 and 1 590 cm^{-1} has never been experimentally demonstrated. We have shown that neither variations in the composition of zinc soaps (e.g. mixtures of fatty acids of different chain length or number of double bonds, or mixtures of metal ions) nor fatty acids adsorbed on pigment particles can account for the broad vibration band. FTIR and XRD analysis on model paint films, however, showed that the zinc carboxylate species must be amorphous, and initial experiments suggest that zinc ionomers prepared from linseed oil may be accurate models for mature binding media.

The exact nature of the carboxylate species—disordered metal soaps or metal carboxylate functionalities covalently linked to the polymerized oil network, or both—is at present unclear. However, it is important to make the distinction between zinc soaps and the broader class of zinc carboxylates in the discussion of chemical processes in paint films. These findings represent a breakthrough in the interpretation of FTIR spectra of oil paint samples. A broadening and shift of the ν_a COO^- band of the metal carboxylate signifies an oil paint system where pigments have partially degraded but metal soaps have not been able to crystallize (yet), i.e. an intermediate stage between an intact and a strongly deteriorated paint film. As such, FTIR analysis provides important information on the internal conditions of oil paint layers and the degree of degradation, aiding conservation treatments of invaluable works of art.

5 Acknowledgements

The authors thank Ella Hendriks (Van Gogh Museum) and Muriel Gelddof (Cultural Heritage Agency, the Netherlands) for making the sample of the Van Gogh painting available. This work is part of the PAinT project, supported by the Science4Arts program of the Dutch Organization for Scientific Research (NWO), and the leadART project, part of the Joint Program Initiative for Joint Research Projects on Cultural Heritage (JPI-JHEP).

References

1 M. Lazzari and O. Chiantore, *Polymer Degradation and Stability*, 1999, **65**, 303–313.
2 C. Higgit, M. Spring and D. Saunders, *National Gallery Technical Bulletin*, 2003, **24**, 75–95.
3 J. van der Weerd, M. Gelddof, L. Struik van der Loeff, R. Heeren and J. Boon, *Zeitschrift für Kunsttechnologie und Konservierung*, 2003, **17**, 407–416.
4 M. J. Plater, B. De Silva, T. Gelbrich, M. B. Hursthouse, C. L. Higgitt and D. R. Saunders, *Polyhedron*, 2003, **22**, 3171–3179.
5 P. Noble, A. van Loon and J. Boon, ICOM Committee for Conservation, 14th Triennial Conference Preprints, The Hague, 12-16 September 2005, London, 2005, pp. 496–503.
6 M. Spring, C. Ricci, D. A. Peggie and S. G. Kazarian, *Analytical and Bioanalytical Chemistry*, 2008, **392**, 37–45.
7 Z. Kaszowska, K. Malek, M. Pańczyk and A. Mikołajska, *Vibrational Spectroscopy*, 2013, **65**, 1–11.
8 K. Keune and J. Boon, *Studies in Conservation*, 2007, **52**, 161–176.
9 K. Keune and G. Boevé-Jones, Issues in Contemporary Oil Paint, 2014, pp. 283–294.
10 J. Sanyova, S. Cersoy, P. Richardin, O. Laprévote, P. Walter and A. Brunelle, *Analytical Chemistry*, 2011, **83**, 753–760.
11 V. Otero, D. Sanches, C. Montagner, M. Vilarigues, L. Carlyle, J. A. Lopes and M. J. Melo, *Journal of Raman Spectroscopy*, 2014, **45**, 1197–1206.
12 L. Robinet and M.-C. Corbeil, *Studies in Conservation*, 2003, **48**, 23–40.
13 J. Hermans, K. Keune, A. van Loon, M. Stols-Witlox, R. Corkery and P. Iedema, ICOM-CC 17th Triennial Conference Preprints, Melbourne, 15-19 September 2014, Paris, 2014, p. art. 1603.
14 G. Osmond, J. Boon, L. Puskar and J. Drennan, *Applied Spectroscopy*, 2012, **66**, 1136–1144.
15 C. Clementi, F. Rosi, A. Romani, R. Vivani, B. G. Brunetti and C. Miliani, *Applied Spectroscopy*, 2012, **66**, 1233–1241.
16 R. Mazzeo, S. Prati, M. Quaranta, E. Joseph, E. Kendix and M. Galeotti, *Analytical and Bioanalytical Chemistry*, 2008, **392**, 65–76.
17 G. Gautier, A. Bezur, K. Muir, F. Casadio and I. Fiedler, *Applied Spectroscopy*, 2009, **63**, 597–603.
18 J. J. Hermans, K. Keune, A. van Loon, R. W. Corkery and P. D. Iedema, *Polyhedron*, 2014, **81**, 335–340.
19 A. Lenz, L. Selegård, F. Söderlind, A. Larsson, P. O. Holtz, K. Uvdal, L. Ojamäe and P.-O. Käll, *Journal of Physical Chemistry C*, 2009, **113**, 17332–17341.
20 I. Dreveni, O. Berkesi, J. A. Andor and J. Mink, *Inorganica Chimica Acta*, 1996, **249**, 17–23.
21 F. Lacouture, J. Peultier, M. François and J. Steinmetz, *Acta Crystallographica C*, 2000, **56**, 556–557.
22 *Van Gogh's Studio Practice*, ed. M. Vellekoop, M. Gelddof, E. Hendriks, L. Jansen and A. de Tagle, Yale University Press, 2013.
23 M. Soucek, T. Khattab and J. Wu, *Progress in Organic Coatings*, 2012, **73**, 435–454.
24 N. Lah, G. Rep, P. Šegedin, L. Golič and I. Leban, *Acta Crystallographica*, 2000, **C56**, 642–643.
25 P. Taheri, T. Hauffman, J. M. C. Mol, J. R. Flores, F. Hannour, J. H. W. de Wit and H. Terryn, *Journal of Physical Chemistry C*, 2011, **115**, 17054–17067.
26 T. Ishioka, K. Maeda, I. Watanabe, S. Kawauchi and M. Harada, *Spectrochimica Acta Part A*, 2000, **56**, 1731–1737.
27 S. Kutsumizu, K. Tadano, Y. Matsuda, M. Goto, H. Tachino, H. Hara,

E. Hirasawa, H. Tagawa, Y. Muroga and S. Yano, *Macromolecules*, 2000, **33**, 9044–9053.
28 M. Coleman, J. Lee and P. Painter, *Macromolecules*, 1990, **23**, 2339–2345.
29 B. P. Grady, *Polymer Engineering & Science*, 2008, **48**, 1029–1051.
30 S. Kutsumizu, H. Tagawa, Y. Muroga and S. Yano, *Macromolecules*, 2000, **33**, 3818–3827.
31 A. M. Castagna, W. Wang, K. I. Winey and J. Runt, *Macromolecules*, 2011, **44**, 2791–2798.
32 G. J. Tudryn, M. V. O'Reilly, S. Dou, D. R. King, K. I. Winey, J. Runt and R. H. Colby, *Macromolecules*, 2012, **45**, 3962–3973.
33 L. M. Hall, M. J. Stevens and A. L. Frischknecht, *Macromolecules*, 2012, **45**, 8097–8108.
34 K.-J. Lin and J. K. Maranas, *Macromolecules*, 2012, **45**, 6230–6240.